

# Deep-Waveform: A Learned OFDM Receiver Based on Deep Complex Convolutional Networks

Zhongyuan Zhao

Cyber-Physical Networking Lab

Department of Computer Science and Engineering

University of Nebraska-Lincoln, Lincoln, Nebraska, USA

Email: zhzhao@cse.unl.edu

**Abstract**—Recent explorations of Deep Learning in the physical layer (PHY) of wireless communication have shown the capabilities of Deep Neuron Networks in tasks like channel coding, modulation, and parametric estimation. However, it is unclear if Deep Neuron Networks could also learn the advanced waveforms of current and next-generation wireless networks, and potentially create new ones. In this paper, a Deep Complex Convolutional Network (DCCN) without explicit Discrete Fourier Transform (DFT) is developed as an Orthogonal Frequency-Division Multiplexing (OFDM) receiver. Compared to existing deep neuron network receivers composed of fully-connected layers followed by non-linear activations, the developed DCCN not only contains convolutional layers but is also almost (and could be fully) linear. Moreover, the developed DCCN not only learns to convert OFDM waveform with Quadrature Amplitude Modulation (QAM) into bits under noisy and Rayleigh channels, but also outperforms expert OFDM receiver based on Linear Minimum Mean Square Error channel estimator with prior channel knowledge in the low to middle Signal-to-Noise Ratios of Rayleigh channels. It shows that linear Deep Neuron Networks could learn transformations in signal processing, thus master advanced waveforms and wireless channels.

**Index Terms**—Wireless Communications, Physical Layer, Deep Learning, Artificial Neuron Networks, OFDM, Modulation

## I. INTRODUCTION

Despite the great success of Deep Learning in a number of fields, its application in wireless communication, especially the physical layer (PHY), was explored only very recently [1]–[9]. Many considered that phenomena in the physical layer of over-the-air wireless communication, such as noise, fading, channel impairment, etc, have been understood, and addressed by well-established theories of signal and coding. On the other hand, although some progresses, such as signal classification, have been achieved in recent works [1]–[9], it is yet unclear if Deep Learning (DL), known as a black box approach good at structured tasks those are easy for human while hard for traditional analytical approaches, would be able to outperform white-box approaches, such as signal and coding theories.

Currently, the applications of DL in wireless communications are mostly focused on enhancing certain functionalities [7], [10]. Above the PHY level, DL is applied in resource management, such as traffic prediction on network level [11], interference alignment [12], as well as decision makings such as power control and spectrum sharing [13]. Among the researches of DL in PHY, many works focus on enhancing

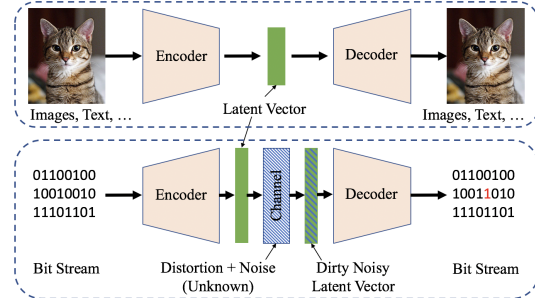


Fig. 1. General AutoEncoder (Top) v.s. Communication AutoEncoder.

certain components in wireless system [7], such as signal classification [1], [2], detection [8], channel coding [3], [5], channel estimation [8], [14], [15], Direction-of-Arrival (DoA) estimation [14], or control problems such as antenna titling. Another thread of researches attempt to establish a novel, end-to-end, communication architecture entirely based on Deep Neuron Networks (DNN) [4], [6], [7].

Among these efforts, building a DL-based end-to-end wireless communication architecture is the most aggressive attempt that could potentially transform the field that is largely based on expert knowledge and models. In [4], [6], the end-to-end wireless PHY is viewed as an autoencoder (AE), as illustrated in Fig. 1. Compared to a typical AE in the DL field that processes structured data such as image and natural language, as shown in Fig. 1, a communication AE has two unique characters: First, the objective of communication AE is to find latent coding that can carry information over detrimental wireless channel, generally by increasing the redundancy, while typical AE is intended to find compact representations of structured data in lower-dimensional latent space without concern of pollution of the code. Second, communication AE is designed to learn the inherent behaviors of channel rather than the structure of data. Data in a communication AE—input and output bits—is considered unstructured and incompressible. Therefore, an communication AE should be trained over a set of channel(s) with random data.

Numerical and experimental evaluations in [4], [6] demonstrate the capability of DNN in learning key PHY functionalities all together, e.g. channel coding, modulation, carrier synchronization. QAM-like constellations different from those designed by experts are created by their AEs. However, none

of these works have shown the ability of DNN in mastering advanced waveforms in modern wireless networks, such as the family of Orthogonal Frequency Division Modulation (OFDM). Furthermore, AEs in [4], [6] have not outperformed expert-designed wireless communication systems.

Building an DNN that work with OFDM signal without using explicit Discrete Fourier Transform (DFT) module is a clear demonstration of the capability of DL in learning (and potentially creating) advanced waveforms. Waveform generation relies on various complex convolutions, such as filter and DFT, on digital base-band signal that is typically represented as complex number—the In-Phase and Quadrature (IQ) data. However, complex convolution is not currently supported by popular Deep Learning platforms, such as TensorFlow [16], Keras [17]. On the other hand, due to the lack of theoretical guidance on using non-linear activations, the extensive usages of Rectified Linear Unit (Relu) [4], [6], [8] seems to contradict with existing, generally linear, signal processing techniques.

In this paper, an OFDM receiver entirely based on Deep Complex Convolutional Network (DCCN) is developed without using any FFT/IFFT modules. The DCCN receiver contains a basic OFDM receiver and a separated channel equalizer. Following the principle of signal processing, the developed DCCN model is significantly different from existing works [4], [6], [8] that only use Fully-Connected hidden layers with Rectified Linear Unit (Relu) activation. Our model contains both dense and convolutional layers which are mostly linear-activated, and new structures of residual and skip connections. Moreover, complex convolutional layer is implemented within Tensorflow [16] to process complex IQ data, instead of treating it as two independent real numbers. The DCCN-based OFDM receiver achieves similar bit error rate (BER) of an expert receiver on 2,4,8, and 16 QAMs in AWGN channel, and learns to exploit the Cyclic Prefix to outperform an LMMSE channel estimator with prior channel information in Rayleigh channels over low to middle SNRs. This work shows the capabilities of Deep Learning in complex signal transformations that are key to master waveforms and channel behaviors.

The rest of this paper is organized as follows: Related work is discussed in Section II. OFDM communication system is introduced in Section III. In Section IV, the model and training approaches of DCCN receiver and equalizer are introduced. Numerical evaluation results are presented in Sections V. Finally, the paper is concluded in Section VI.

## II. RELATED WORK

### A. Deep Learning in PHY of Wireless Communications

Deep learning for wireless communication in physical layer emerged only lately. In surveys [7], [10], it is pointed out that Deep learning could be used for modulation recognition, channel decoding, and detection to enhance existing wireless communication system, and can also be used to construct novel communication architecture, extend existing expert knowledge, for multi-user and MIMO. In [1], a convolutional (Conv) network is developed to classify the modulation of radio signal. In [2], a Radio Transformer Network (RTN) based on

Conv and FC layers with Relu activations is developed for parametric estimation and recover signal, e.g. from Carrier Frequency Offset (CFO). Despite Complex Convolutional (C-Conv) layer is introduced in [2], it is not used in RTN, in which complex number is represented by power and phase but real and imaginary parts. For many tasks, this representation could be problematic as the phases of two nearby samples may jump from  $-\pi$  to  $\pi$ . An end-to-end wireless communication architecture based entirely on DNN is introduced in [4], where the entire PHY is viewed as an autoencoder trained by unsupervised learning. The Deep Learning PHY is expanded to multiple-input multiple output (MIMO) system in [5] by introducing spatial-temporal coding. The DNN models in [4], [5] are both based on dense (Fully-Connected (FC)) layers, normalization, and activations such as Relu and Softmax. Channel State Information (CSI) is estimated in [5] via FC layers with Relu activation at the receiver. In [3], Deep Learning based channel encoding is explored in AWGN channel with impairment. Comparison in [3] shows that DNN networks (Fully-Connected Layers) always outperform or equal to CNN networks (network with Convolutional (Conv) layers). In [6], an DL based end-to-end communication system is developed, where dense layers with Relu are used at both transmitter and receiver. However, the resulted BER performance in [6] underperforms existing DQPSK in both AWGN simulation and real channels. In [18], an OFDM end-to-end autoencoder based on FC layers and DFT/IDFT is claimed to outperform the QPSK with MMSE channel estimation in block error rate (BLER). However, to the best of our knowledge, learning advanced waveforms have not been addressed in all those works.

### B. OFDM System and Its Enhancements

OFDM system is the most popular system in modern wireless communication. In [19], [20], the OFDM physical layer and various channel estimation approaches are introduced. Any improvements on OFDM system would significant impact the existing wireless system. Several enhancements is proposed to improve OFDM system, such as , Filter Bank MultiCarrier (FBMC), UFMC, GFDM [21] for next generation communication system such as 5G. These new waveforms are generally modifications of OFDM for better characteristics with regards to various interferences. An constellation enhancement approach [22] and DL-based coding system [23] are proposed to reduce the Peak to Average Power Ratio (PAPR) of OFDM waveform.

At the receiver side, several works explored the use of Cyclic Prefix (CP) to enhance the performance of OFDM receiver [24]–[27]. CP is a redundancy of time-domain OFDM symbol which is necessary to mitigate intersymbol interference (ISI), but takes up a portion of spectrum resource in time domain. A key of exploiting CP is to determine the unpolluted length in CP. Our work is a complementary of existing analytical approaches, such as Maximum Likelihood [24], [26], Factor Graph [25], [27] in exploiting CP.

Several recent works focus on DL-based enhancements of OFDM receiver [8], [9]. In [8], an 5-layer DNN-based OFDM

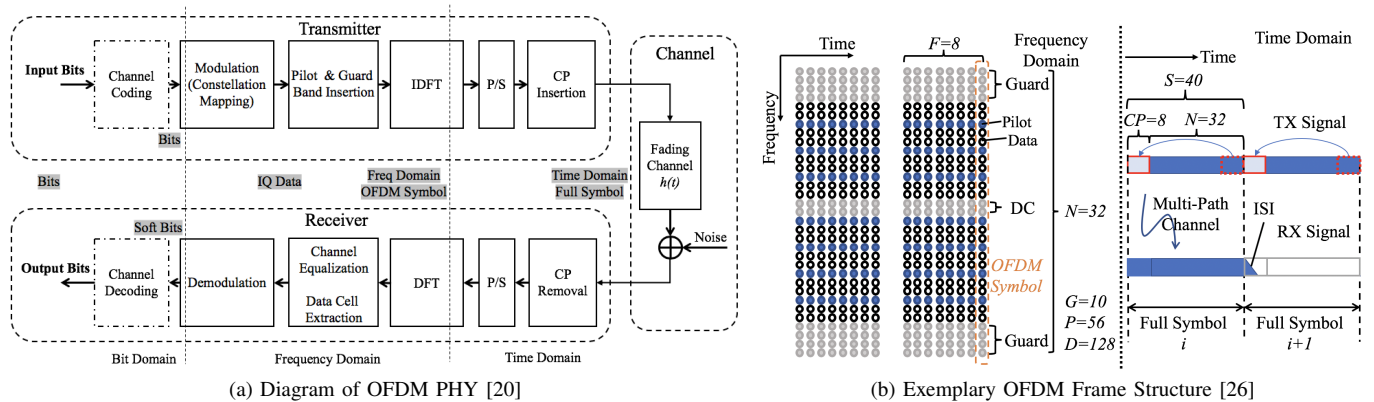


Fig. 2. OFDM Communication System Physical Layer.

receiver simultaneously implements channel estimation and modulation symbol recovery. Their model uses Relu activation for hidden layers, and sigmoid for output, and equalization and recovery are trained in 2 stages. However, channel equalizer and receiver are separated in this paper, and our receiver directly output bits instead of IQ data. Moreover, [8] only studies QPSK modulation with a specific block type pilot, which we find could not work on higher order modulation. A DL-based OFDM receiver in [9] is claimed outperforming LMMSE channel estimator by initialized to known model. However, explicit usage of FFT/IFFT [9], [18], [23] could not demonstrate the ability of DNN in learning waveforms.

### III. OFDM COMMUNICATION SYSTEM

The physical layer (PHY) of OFDM communication is introduced in this section. Specifically, the transmitter, receiver, channel process, and channel equalization in expert system are introduced to serve as the baseline of this paper.

#### A. Physical Layer

The block diagram of the PHY of OFDM communication system is illustrated in Fig. 2(a). Input bits of the OFDM transmitter is first encoded (with redundancy) to reduce errors in specific channels, the encoded bits are mapped into constellation on the In-Phase and Quadrature (IQ) plane via modulation, the resulted IQ data is represented as complex number. Pilot and guard bands are inserted to the IQ data to form frequency-domain OFDM symbol. The frequency-domain OFDM symbol is then transformed into time-domain via Inverse Discrete Fourier Transformation (IDFT), and then converted in to 1 dimensional (1D) via Parallel to Serial (P/S) conversion. Cyclic Prefix (CP), which is a section of time-domain IQ data from the end, is copied to the beginning of time-domain IQ data to form a full time-domain OFDM symbol, as shown in Fig. 2(b). The base-band IQ data stream is then up-converted to radio frequency (RF) and broadcast over-the-air by RF frontend. The radio wave propagated over wireless channel is received and down-converted into base-band digital IQ data by the RF frontend of receiver. A carrier synchronizer recovers time-domain OFDM symbols, and send it to base-band receiver. At the receiver, CP is first removed and rest of the IQ data is transformed to frequency domain via

FFT. A channel equalizer estimates the responses of channel, and equalize the received IQ data distorted by the fading channel. Next, the equalized frequency-domain IQ data is demodulated to soft bits (float numbers), which are further decoded by channel decoder into binary bits. The output bit stream is sent to next layer and recovered into packets. Note that channel equalization is for fading rather than AWGN channel. Moreover, channel coding is ignored in this paper in order to focus on the lower PHY.

OFDM communication system is usually based on physical frame composed by multiple OFDM symbols, as illustrated by an example in Fig. 2(b). The notations of parameters in a OFDM frame are defined as follows: OFDM symbol contains  $N$  subcarriers, where  $N$  is the size of IDFT at transmitter. Among these  $N$  subcarriers, there are total of  $G$  guard subcarriers at the center (DC guard band) and edge (edge guard band). A OFDM frame contains multiple consecutive OFDM symbols, which is denoted as  $F$ . A resource cell refers to a subcarrier of an OFDM symbol. For each OFDM frame, there are  $P$  cells allocated as training signals (pilot) known by both transmitter and receiver, and the rest  $D$  cells allocated to modulated IQ data. Moreover, in time domain, cyclic prefix (CP), which is a copy of a section of time-domain OFDM symbol, is added to the beginning of each OFDM symbol. As a result, the total length of time-domain OFDM symbol will be increased from  $N$  to  $S$ . These parameters are usually prescribed according to channel characteristics, such as coherence time, coherence bandwidth, and total channel bandwidth. Meanwhile, for  $m$ -ary modulation, each constellation points contains  $m$  bits, and there are  $2^m$  constellation points.

#### B. Wireless Channel

From the perspective of digital base-band, the wireless channel not only include over-the-air propagation between transmit and receive antennas, but also everything on the RF frontend. However, in this paper, we only consider a wireless channel with fading and noise processes, as a well accepted simplification [20]. The wireless channel is modeled as:

$$y = x * h + n, \quad (1)$$

where vectors  $x$  and  $y$  are time-domain transmitted and received signals, vector  $h$  is time domain channel coefficient,

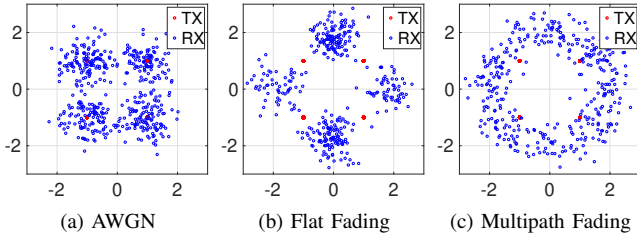


Fig. 3. The Effects of Different Wireless Channels on QPSK Modulation, SNR 6dB, on IQ Plane (x: In-Phase, y: Quadrature).

vector  $n$  is time domain white noise, and  $*$  stands for convolution. (1) can also be represented in frequency domain as:

$$Y = X \odot H + N_o, \quad (2)$$

where the vector  $X$ ,  $Y$ ,  $H$ , and  $N_o$  are frequency domain transformation of  $x$ ,  $y$ ,  $h$ , and  $n$ , e.g.  $X = DFT(x)$ .  $N_o$  is still white noise.  $\odot$  stands for element wise production. Fading channel is modeled as a tapped delay line, in which channel responses,  $h$ , are a train of impulse responses [20]:

$$h(t, \tau) = \sum_{i=0}^{K-1} h_i(t) \delta(\tau - \tau_i), \quad (3)$$

where the  $i$ th tap,  $h_i(t)$ , is a complex number representing amplitude and phase of the  $i$ th path of signal propagation, and  $\sum_{i=0}^{K-1} ||h_i(t)||^2 = 1$ . The fading coefficients varies by radio environments. Fading is called slow fading if the channel coefficients keep relatively constant within a frame, vise versa fast fading. Although theoretically, channel coefficient can also change within an OFDM symbol, this situation is usually not considered based on the assumption that the OFDM frame parameters are carefully selected before hand based on prior knowledge of wireless channel.

$K$  in (3) stands for number of propagation paths in the channel. For an OFDM symbol, if  $K = 1$ , channel coefficients would be constant across all the sub-carriers, the channel is flat fading. If  $K > 1$  (multipath), channel coefficients may vary across sub-carriers, the channel is frequency selective. In Rayleigh channel, the real and imaginary parts of  $h_i$  follow identically independent Gaussian distributions, and  $||h_i||^2$  follows Rayleigh distribution. The effects of different fading on OFDM frame in frequency domain are illustrated in Fig. 3. Note that only noise and fading are considered, while channel impairment for channel coding is left for future works.

The multipath propagation introduces Inter-Symbol Interference (ISI) at the receiver, as shown in Fig. 2(b). To mitigate ISI, proper length of Cyclic Prefix is selected such that ISI from OFDM symbol  $i$  only stays in the CP of OFDM symbol  $i+1$  in the worst cases. CP is usually dropped out at the OFDM receiver to eliminate ISI. However, not all the CP is polluted by ISI in most cases, therefore, the CP, as a redundancy of main signal, can be exploited to improve the receiver performance. This work shows that except existing analytical approaches [24]–[27], exploiting the CP to enhance receiver performance can be learned by DCCN.

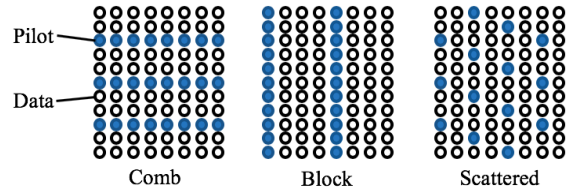


Fig. 4. Typical OFDM Pilot Patterns: Comb, Block, and Scattered.

### C. Channel Estimation and Equalization

In communication system, training signal (pilot) is inserted to the frames so that the receiver could estimate the channel responses, based on the assumption that pilot and data are distorted similarly. A proper pilot pattern is designed to meet such assumption. Typical pilot patterns in OFDM system are: block, comb, and scattered, as shown in Fig. 4 [20]. The pilots could be a constant value on IQ plane, or known sequence with low auto-correlation (e.g. LTE system). The simplest channel equalization in OFDM system is based on Least Square (LS) estimator [19], [20]:

$$\hat{X}_D = \frac{Y_D}{f(\hat{H}_P)}, \quad \text{where } \hat{H}_P = \frac{Y_P}{X_P}, \quad (4)$$

where  $X_P$  and  $Y_P$  are transmitted and received pilots in frequency domain, respectively, and  $Y_D$  and  $\hat{X}_D$  are received data and recovered transmit data, respectively. The channel coefficients of data cells are obtained by interpolation,  $f(\cdot)$ , of channel estimates on pilot  $\hat{H}_P$ . Common interpolations include linear, spline, low-pass-filter, and DFT [19], [20]. Other estimators, such as Minimum Mean Square Error (MMSE), Linear MMSE (LMMSE), Maximal likelihood, and parametric channel modeling-based (PCMB) estimator, are based on LS estimation and/or prior channel knowledge [19], [20].

## IV. DCCN-BASED OFDM RECEIVER

In this section, the design and training approaches of the Deep Complex Convolutional Network (DCCN)-based OFDM receiver are introduced. The DCCN-based OFDM receiver contains a basic OFDM receiver without channel equalization, and a separate channel equalizer. The design of the basic OFDM receiver and channel equalizer are inspired by expert OFDM receiver and LS channel equalizer. Therefore, the design of flow-graph is described as function blocks of expert OFDM receiver and LS channel equalizer. However, the actual behavior of each layer of a trained model may be different from the designed purpose. Rather than specifying the functionality of each layer, this design approach is to ensure a basic LS estimator is at least in the search space of deep learning by leveraging field knowledge. In fact, the design is to contain rich computational redundancy, hoping that some unknown solution or phenomenon may be learned or discovered. After training, most redundancy would be removed, and skip connection structure is to give the DCCN model maximal flexibility to achieve best performance.



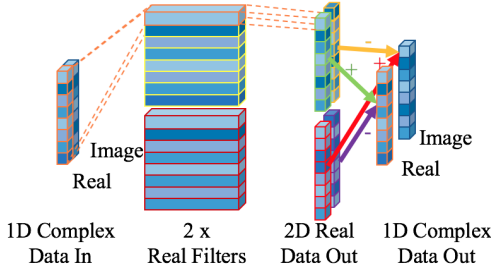


Fig. 5. Implementation of a 1D Complex Number Conv Layer ( $8 \times 8 \times 1$ ) based on a 2D Real Number Conv Layer ( $16 \times (1, 8) \times 1$ )

### A. Complex Layers

Currently (Oct, 2018), complex neuron network is not yet supported by popular Deep Learning platforms. For example, Tensorflow [16] and Keras [17] only supports untrainable complex operations, such as FFT, and IFFT, but not supports complex numbers in trainable Neuron Network layers, like fully-connected (FC), and convolutional (Conv) layers. The construction of complex neuron networks is addressed in [28]. The major concern is complex multiplication:

$$(a + bi) \times (c + di) = (ac - bd) + (ad + bc)i. \quad (5)$$

For a minimal FC complex layer with input and output both of size 1, consider its input as  $a + bi$  and weight as  $c + di$ . Based on (5), the complex FC layer can be implemented by real FC layer with input and output both of size 2. The 4 weights of the real FC layer are able to be trained to be  $c, -c, d, -d$ . Therefore, a real FC layer is capable of implementing a complex FC layer of half size. A complex Conv layer can be implemented by a higher dimensional real conv layer with double filters [1]. As illustrated in Fig. 5, an 1D complex Conv layer of size  $8 \times 8 \times 1$  (which stands for 8 filters, each with a size of 8, and channel of 1) can be implemented by a 2D real conv layer of size  $16 \times (1, 8) \times 1$ . In this work, real and imaginary parts of a complex tensor are in the last dimension.

Digital Signal Processing in OFDM system is generally linear transformation (on complex numbers). Moreover, the real and imaginary parts of IQ data are in both positive and negative regimes. Therefore, we only use tanh activations for IQ data by treating a complex number as two independent real numbers. Non-linear operations are between bit and IQ domains, such as modulation and demodulation. In demodulation, IQ data is simply viewed as 2 real numbers, and Leaky Rectified Linear Unit (LRelu) is used only for real numbers.

### B. Basic DCCN Receiver

The basic DCCN receiver is an OFDM receiver without channel equalizer. The flow graph of basic DCCN receiver is illustrated in Table I. The DCCN receiver model contains three parts: the first part includes first 3 layers, which is intended to transform time-domain OFDM symbol into frequency domain. The major component of the first part is a Complex Conv (C-Conv) layer of size  $N \times S(N) \times 1$ . The basic DCCN receiver can take in or drop CP by configuration. Dropping CP is implemented by an optional slice operation before the

Table I. Basic DCCN OFDM Receiver Flow-Graph

| Layer       | Type                                      | Output Shape      |
|-------------|---|-------------------|
| Input       | Batch_Normalization                       | $[B, F, S, 2]$    |
| (CP-Drop)   | Slice (Optional)                          | $[B, F, N, 2]$    |
| DFT-Like    | Complex 1D-Conv, $N \times S(N) \times 1$ | $[B, F, N, 2]$    |
| Reshape0    | Reshape                                   | $[B, 2FN]$        |
| Extraction  | Fully-Connected                           | $[B, 2D]$         |
| IQ_Data     | Reshape                                   | $[B, D, 2]$       |
| Const1      | Real Conv, $2^m \times 1 \times 2$        | $[B, D, 2^m]$     |
| Const2      | Real Conv, $2^m \times 1 \times 2^m$      | $[B, D, 2^m]$     |
| Activation0 | Leaky Relu                                | $[B, D, 2^m]$     |
| Concat      | Concatenate (IQ_Data, Activation0)        | $[B, D, 2^m + 2]$ |
| Demod       | Fully-Connected                           | $[B, D, 2m]$      |
| Activation1 | Leaky Relu                                | $[B, D, 2^m]$     |
| Reshape2    | Reshape                                   | $[B, D, m, 2]$    |
| Output      | Softmax                                   | $[B, D, m, 2]$    |

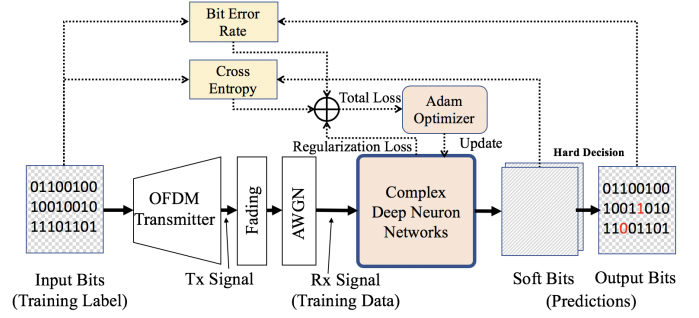


Fig. 6. Block Diagram of DCCN Training System.

C-Conv layer. The second part contains layers 4 to 6, which is intended to extract all the data cells of an OFDM frame, this is implemented by a FC layer. Parts 1 and 2 parts are for processing IQ data (complex number), of which the real and imaginary parts are stored in the last dimension of tensors. Part 3 is for demodulation, which is convert the complex IQ data into soft bits. Part 3 treat the real and imaginary parts of complex IQ data as 2 channels of real number. The IQ data is fed to 2 Real Conv (R-Conv) layers with  $2^m$  filters, followed by a LRelu activation. A skip connection is designed to combine the original IQ data and the output of LRelu activation, and feed them together to a final FC layer. The FC layer is followed by an LRelu activation and then an softmax activation. The output of softmax activation are soft bits, which represents each bit with 2 real numbers (e.g. Log-Likelihoods of 0 and 1).

Since channel coding is out of the scope of this paper, we simply use hard decision to get output bits from the soft bits. The cross entropy and bit error rate (BER) are then calculated from soft bits and output bits by comparing with input bits. The cross entropy and BER are used to construct loss function for training of the DCCN models, as shown in Fig. 6.

### C. DCCN Channel Equalizer

The channel equalizer of OFDM receiver is usually located in frequency domain, (Fig. 2(a)) to avoid convolution operation. In this work, a standalone equalizer is designed before the basic receiver for the convenience of implementing transfer learning (detailed in Section IV-D) in Tensorflow [16]. The

Table II. DCCN Equalizer Flow-Graph

| Layer        | Type  | Output Shape      |
|--------------|---|-------------------|
| Input        | Layer Norm, (per frame)                     | $[B, F, S, 2]$    |
| (CP-Drop)    | Slice (Optional)                            | $[B, F, N, 2]$    |
| Reshape0     | Reshape                                     | $[B, F, 2S(N)]$   |
| CP_Process   | Fully-Connected                             | $[B, F, 2N]$      |
| Reshape1     | Reshape                                     | $[B, F, N, 2]$    |
| DFT-Like     | 1D Complex Conv, $N \times N \times 1$      | $[B, F, N, 2]$    |
| Reshape2     | Reshape                                     | $[B, 2FN]$        |
| Pilot        | Fully-Connected                             | $[B, 2P]$         |
| Est0         | Fully-Connected, input: Pilot               | $[B, 2P]$         |
| Est1         | Fully-Connected, input: Pilot-Est0          | $[B, 2P]$         |
| Est2         | Fully-Connected, input: Est0-Est1           | $[B, 2P]$         |
| Est3         | Fully-Connected, input: Est1-Est2           | $[B, 2P]$         |
| Est4         | Fully-Connected, input: Est2-Est3           | $[B, 2P]$         |
| Concat       | Concatenate (Pilot, Est0, ..., Est4)        | $[B, 12P]$        |
| Interpolate0 | Fully-Connected, activation: tanh           | $[B, 2FN]$        |
| Interpolate1 | Fully-Connected, activation: tanh           | $[B, 2FN]$        |
| Interpolate2 | Fully-Connected, activation: tanh           | $[B, 2FN]$        |
| Reshape3     | Reshape                                     | $[B, F, N, 1, 2]$ |
| 2D-Filter    | 2D Complex Conv, $1 \times (F, N) \times 1$ | $[B, F, N, 1, 2]$ |
| Estimates    | Reshape                                     | $[B, F, N, 2]$    |
| Equalization | Complex Division: DFT-Like/Estimates        | $[B, F, N, 2]$    |
| IDFT-Like    | 1D Complex Conv, $N \times N \times 1$      | $[B, F, N, 2]$    |
| Reshape4     | Reshape                                     | $[B, 2FN]$        |
| CP_Handle    | Fully-Connected                             | $[B, 2FS]$        |
| Output       | Reshape                                     | $[B, F, S, 2]$    |

flow graph of the equalizer, as presented in Table II, contains 4 parts by design. The first (layer 0-5) and fourth parts (last 4 layers) are DFT/IDFT-like complex Conv layers intended to perform time/frequency domain transformation. Notice that in part 1, a FC layer is placed before the DFT-Like layer to process CP. In part 4, the IDFT-Like layer is followed by a FC layer for adding back CP. Part 2, from layers 6 to 19, is for channel estimation. Part 3, layer 20, is frequency domain channel equalization implemented by complex division: the output of part 1 (frequency domain receive signal) over the output of part 2 (channel estimates).

In part 2, the channel estimator, the first step is extract pilot in a frame with FC layer, followed by a FC layer for LS estimation. Next, 4 layers of FC layers are followed to estimate the residual of previous estimation. The layers of pilot, 1st order LS estimation, and 4 residual estimations are all fed into next Interpolation block through a skip connection structure (Concat). The interpolation block contains 3 FC layers with tanh activation of full frame size, followed by a 2D complex Conv layer of size  $1 \times (F, N) \times 1$  (1 filter with size  $(F, N)$  and 1 channel), as 2D-Filter. The output of the 2D Filter is reshaped to match the size of frequency domain signal from part 1. Through experiments, we found that similar model without the residual components and skip connections would have significantly worse performance.

For a particular CP option, the same DCCN flow graph is used for all modulations and fading settings, but trained separately, hence end with different parameters. The only difference between CP options is whether or not dropping the CP in part 1 of the DCCN equalizer flow-graph.

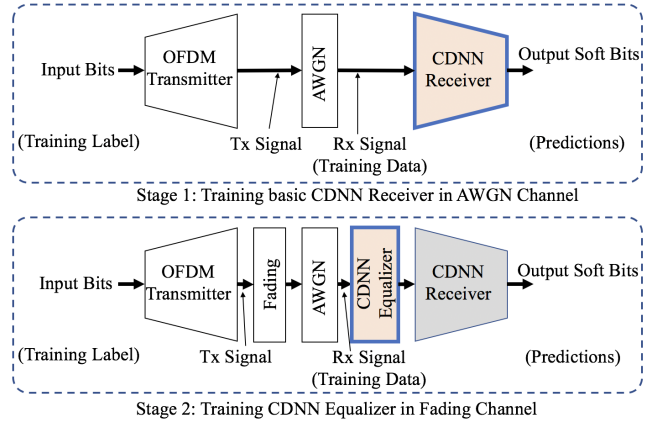


Fig. 7. 2-Stage Transfer Learning for Training The Receiver and Equalizer.

## D. 2-Stage Training

The training setting of DCCN receiver, as illustrated in Fig. 6, contains an online random generator creating random bits as training labels, a OFDM transmitter translate input bits into time domain OFDM symbols (transmit (Tx) signal). A channel model adds fading and noise to the Tx signal to create receive (Rx) signal. The Rx signal is the training data fed into the DCCN model. The output of DCCN model are soft bits, and output bits are generated by hard decision. The cross entropy and BER are calculated based on training labels and predictions (Soft bits and output bits). The total loss,  $L$ , is calculated by sum of the cross entropy (CE), logarithmic BER, and regularization loss ( $L_{reg}$ ) of the model:

$$L = CE + \log_{10}(BER) + L_{reg} . \quad (6)$$

The logarithmic BER could prevent diminishing gradient due to tiny changes of CE when BER is very small. With the loss function, Adam optimizer runs back-propagation to optimize randomly initialized DCCN model during training.

The equalized DCCN receiver is too complex to be trained together at one time. At best, it takes several times longer than training them separately. Most likely, it never start to converge. Therefore, transfer learning is adopted to train the DCCN receiver and equalizer in two stages, as illustrated in Fig. 7. In stage 1, the basic DCCN receiver is trained in AWGN channel. Fading is removed from channel model in the generation of training data, Rx Signal. When training is completed, the trained DCCN receiver (flow graph with parameters) is saved, and the TensorFlow session is closed. In stage 2, a second TensorFlow session is first initialized for graph-editing. The pre-trained basic DCCN receiver is loaded, and a new model of DCCN Equalizer is built and inserted before the trained DCCN receiver. Then, the edited flow-graph is saved and the second session is closed because graph editing and training have to be in different sessions. After that, a third session is initialized and the previous flow graph is loaded for training. The same cost function is used in stages 1 and 2. At stage 2, fading is included in the generation of training data, and only the DCCN equalizer is trained. The graph-editing

technique enables the DCCN receiver to pass the gradients in back-propagation without being updated in stage 2.

To improve the training efficiency, several techniques are used. First, the training data is fed to the model in mini batches. The batch size is set to 512 OFDM symbols (64 OFDM Frames). With mini-batch technique, we could leverage the high throughput parallel processing capability of GPU, while minimize its high IO latency. Second, in the programming of NumPy-based OFDM transmitter and fading modules, data processing are vectorized and large loops are avoided. Third, the learning rate is set to 0.001 initially and decay exponentially every 2.5 episodes. This ensures a smaller learning rate for fine-tuning the model at later phase of training. Beside setting a maximum number of training episodes, we also set an early stop mechanism to end the training if key performance metric (BER) was not improved in a fixed window of most recent episodes. Notice that since we could not use all the possible training labels ( $2^{46m}$  bits) for training, but generate random bits for each episode, we use episode instead of epoch (an iteration that all training data went through once) throughout this paper.

### E. Training Signal-to-Noise Ratio

There is no clear guidance of setting the training SNR for a DL-based PHY. SNR of 5dB is recommended in [3]. In this paper, we found that relatively low training SNR (e.g. 3dB EbNo) generally helps to achieve better performance with less training. Noise helps to regularize Artificial Neural Networks to avoid over-fitting. However, only low training SNR may hide some flaws of the model. For example, a flawed model maybe trained to contain an small systematic error which outputs slightly more 1s than 0s. At lower SNRs, this systematic error is hidden by relatively large BER. However, such bias will persist and cause a BER floor in high SNR regime.

To minimize systematic error, a combination of low and high SNR setting are used in training. For  $m$ -ary modulation, the base SNR is set as  $3m$  dB. At stage 1, for every 8 OFDM frames, there are 4 frames with SNR of  $3m$  dB, 1 frame of  $3m-3$  dB, and 3 frames of  $3m+5$  dB. This combination helps to improve the training efficiency while minimize systematic errors. At stage 2, the SNR offsets are  $[-3, 0, 0, 3, 6, 9, 12, 17]$  dB for every 8 OFDM frames in training. Under this configuration, the channel estimator is exposed to a wide range of SNR during training. This is because pilot signal carries different amount of channel information at different SNRs, channel estimator trained at a narrow range of SNR is more likely to be over-fitted to a specific SNR range.

## V. EVALUATION RESULTS

The performance of DCCN receiver is evaluated by its bit-error-rate (BER) in different channel and SNR settings. First, the BER of basic DCCN receiver in Additive Gaussian White Noise (AWGN) channel is presented, followed by the BER of equalized DCCN receiver in two Rayleigh fading channels: flat fading and multipath fading.  $m$ -QAM modulation ( $m \leq 4$ )

Table III. Configurations of The Evaluated OFDM System

|                   |  |
|-------------------|--|
| Sample Rate       | 10 Msps                                      |
| Frame Size        | $F = 8$ OFDM Symbols                         |
| FFT Size          | $N = 64$                                     |
| CP Length         | $CP = 16$                                    |
| Guard Band        | $G = 10$ : 4 upper band, 4 lower band, 2 DC  |
| Pilot Cell /Frame | $P = 64$                                     |
| Data Cell /Frame  | $D = 368$                                    |
| PAPR Limit        | 8 (9 dB)                                     |
| Pilot Pattern     | Scattered                                    |
| Pilot Value       | $1 + 1i$ , equal to peak constellation power |
| Modulation        | BPSK, QPSK, 8-QAM, 16-QAM (Gray code)        |
| Fading Model      | Rayleigh: (1) Flat, (2) Multipath (EPA [30]) |
| Channel Coherence | Slow Fading, channel taps updated per frame  |
| CFO               | 0 Hz   |

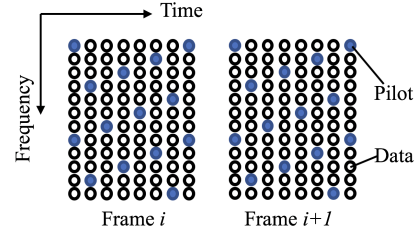


Fig. 8. Scattered Pilot Covers All SCs in a Frame with 8 Cells Per Symbol.

are evaluated. There are 2 options for the basic and equalized DCCN receivers: with and without Cyclic Prefix. A model for each modulation and CP option is built, trained, and tested. The DCCN receivers are benchmarked by an expert OFDM receiver, as shown in Fig. 2(a), implemented in Matlab [29].

The OFDM system and fading channel are configured as in Table III. The sample rate is 10Mbps. An OFDM frame contains 8 OFDM symbols with FFT size of 64 and Cyclic Prefix (CP) length of 16. Each OFDM symbol has 10 guard subcarriers (SCs) including Direct Current (DC), 8 pilot SCs and 46 data SCs. The numbers of pilot and data cells in each frame are 64 and 368, respectively. Pilots are scattered and spread across all non-guard SCs, as illustrated in Fig. 8. This pilot pattern is efficient in spectrum resources, and ensures consistent performance of benchmark channel estimation algorithms, as apposed to other types [8]. Each pilot has value of  $1 + 1i$ . The maximal power of the constellation for a given modulation is normalized to pilot power. Gray code is applied for mapping between constellation and bits. After the transmitter, the Peak to Average Power Ratio (PAPR) of OFDM waveform is limited to 9dB. The AWGN and Rayleigh channels are tested. Fading channel includes flat fading and multipath fading, the latter is Extended Pedestrian A model (EPA) from 3GPP [30]. Slow fading is considered, in which the channel taps are updated per frame. With EPA model, there would be InterSymbol Interference (ISI) within a frame, but no ISI across frames which could be eliminated by the gap slot between 2 frames. The delay spread of EPA model (450 ns) is shorter than CP (1600 ns). For simplicity, perfect synchronization is considered at receiver, so that time and frequency offsets, as well as Doppler shifts are ignored, which are already addressed in [2], [6]. This configuration emulate a baseline scenario of LTE system. For fading channel, the



Table IV. Training Configurations for  $m$ -ary Modulation

| Setting                       | DCCN Receiver                                 | DCCN Equalizer            |
|-------------------------------|---|---------------------------|
| Maximum Episodes              | $1200m$                                       | $4000m$                   |
| Early Stop Window             | 200 episodes                                  | 200 episodes              |
| Initial Learning Rate         | 0.001   | 0.001                     |
| Learning Rate Decay           | Exponential, Rate 2%, Step 500 (2.5 episodes) |                           |
| Baseline SNR (dB)             | $3m$  | $3m$                      |
| $\Delta$ SNR in 8 Frames (dB) | -3, 0, 0, 0, 0, 5, 5, 5                       | -3, 0, 0, 3, 6, 9, 12, 17 |
| Training Bits / episode       | $102400 \times 46 \times m$ bits              |                           |
| Batch Size                    | $512 \times 46 \times m$ bits                 |                           |
| Testing Bits per SNR          | $160000 \times 46 \times m$ bits              |                           |
| Test SNR Points               | -10 to 29 dB, step: 1 dB                      |                           |
| Optimizer                     | SGD with Adam                                 |                           |

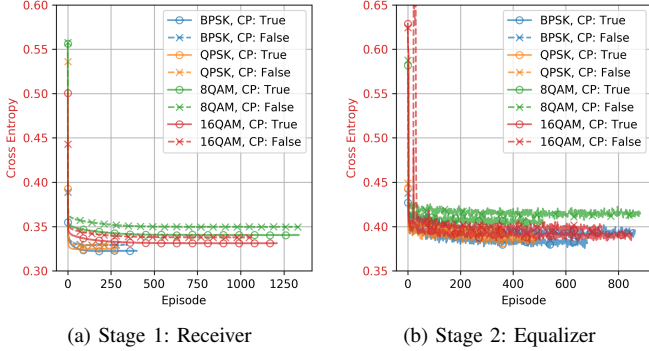


Fig. 9. Training of DCCN Models: Cross Entropy by Episodes

noise power is set according to SNR based on the average signal power of 64 OFDM frames (512 OFDM Symbols).

The configurations for the training of DCCN receiver and equalizer with  $m$ -ary modulation are detailed in Table IV. Stochastic gradient descent-based Adam optimizer with mini batch size of 64 frames are used. For each episode, a new random bit stream (training labels) is generated and converted into corresponding training data by expert OFDM transmitter and channel model. Since training labels are completely random, the total cost for early stop is based on training data rather than a separate test data set. The training ends either when reach to the maximum number of episodes, or the total cost was not improved over the most recent 100 episodes (early stop window). The learning rate is set to 0.001 initially and decayed by 2% every 500 steps or 2.5 episodes. SNR is set per frame based on baseline SNR of  $3m$  dB with different  $\Delta$  values per 8 frames. Each training episode contains 200 mini batches, and testing bits of 2000 frames for each of 40 SNR points (-10 to 29 dB with 1 dB step).

Training a DCCN model takes from 250 to 1300 episodes, as shown in Fig. 9. The training process starts with a quick fitting followed by a long fine-tuning phase: the cross entropy decreases drastically in the first 10-50 episodes, then slowly but steadily until hitting a floor.

#### A. Additive Gaussian White Noise Channel

The BER performance of basic DCCN receivers in AWGN channel over the full range of testing SNR is presented in Figs. 10. The benchmark is Matlab-based expert OFDM receiver without equalizer [29]. The basic DCCN receiver with CP

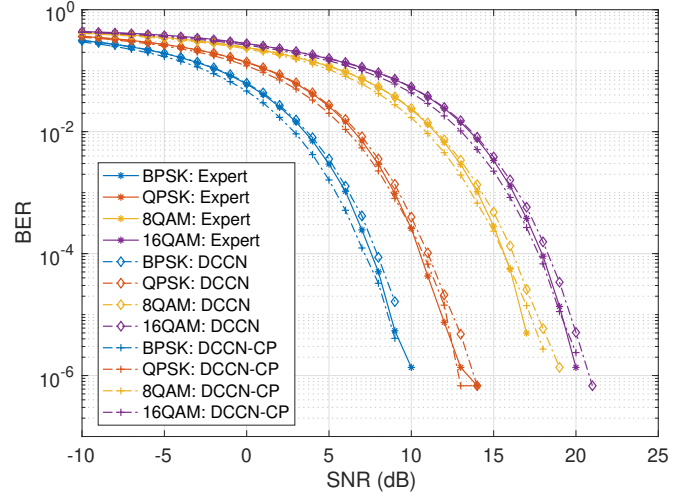


Fig. 10. BER of DCCN Receiver by SNR in AWGN Channel, benchmarked by expert OFDM receiver.

outperforms the benchmark, while DCCN without CP slightly underperforms in high SNRs.

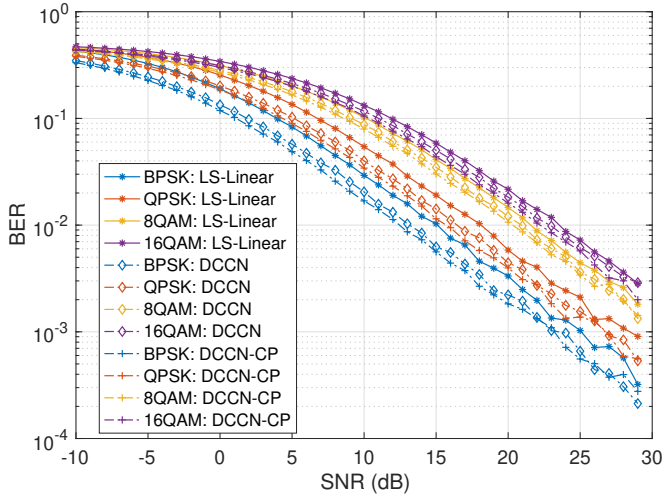
For DCCN receiver without CP, denoted as DCCN, the BER performance is 0.3 to 0.8 dB worse than the benchmark at high SNRs. Note that when BER is very small, e.g.  $\leq 10^{-5}$ , it is more subjected to randomness due to limited test data size. For DCCN receiver with CP, denoted as DCCN-CP, the BER performance is 0.4 to 0.8 dB better than the benchmark, but the improvement diminishes in high SNRs ( $E_b/N_0 \geq 5$  dB). As a redundancy of time-domain OFDM waveform, CP carries some information for all subcarriers while experience independent random noise. Theoretically, CP could improve the signal power by  $CP/N$ , translated into 0.97 dB of improvement in AWGN with our configuration. The test BER of DCCN-CP receiver is about 0.7-0.97 dB better than the DCCN receiver. It can be observed that DCCN of 8-QAM is slightly worse than other modulations in high SNRs. This is probably because 8-QAM constellation is less symmetric than the other 3 modulations.

#### B. Rayleigh Fading Channels

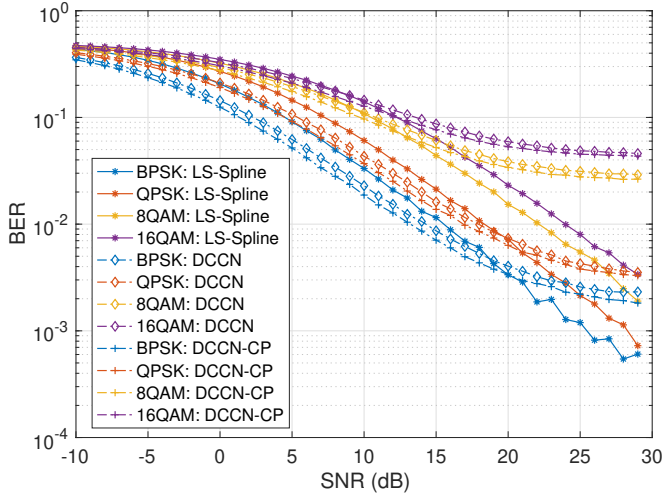
The equalized DCCN receivers are benchmarked by expert OFDM receiver with LS estimators, with 2D linear (flat fading) and 2D Spline (EPA) interpolations, as shown in Figs. 11. In multi-path fading, Spline outperforms linear interpolation, and vice versa in flat fading, as shown in Figs. 12.

The BER of equalized DCCN receivers by SNR in flat fading channel is presented in Fig. 11(a). The equalized DCCN receiver significantly outperforms benchmark in BPSK modulation by 2 to 2.5 dB w/o CP and 2.5 to 3 dB w/ CP. For QPSK, the improvement is 1 to 2 dB w/o CP and 2 to 2.8 dB with CP. For 8QAM and 16QAM, equalized DCCN outperforms benchmark by 0.5 to 1 dB w/o CP and 0.8 to 1.5 dB w/ CP. The improvement also varies by SNR: the DCCN outperforms benchmark by 3 to 5 dB in the negative SNR regime, while the advantage slightly reduced in high SNR





(a) Flat Fading, Benchmark: LS with linear Interpolation

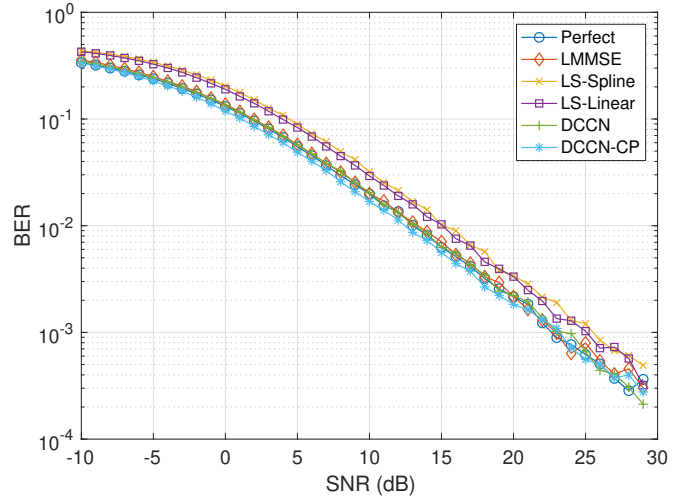


(b) Multipath Fading (3GPP-EPA [30]), Benchmark: LS with Spline

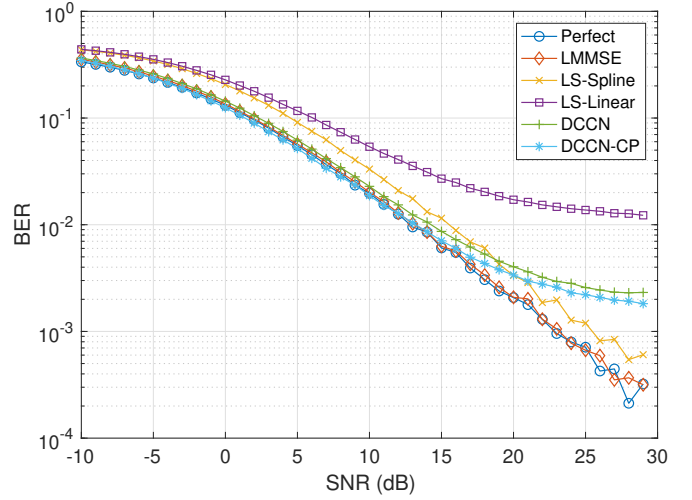
Fig. 11. BER of Equalized DCCN Receiver in Rayleigh Channels, benchmarked by expert OFDM receiver with Least Square channel equalizer.

regime ( $\geq 24\text{dB}$ ). The performance deterioration of DCCN in high SNR regime is contributed by both basic receiver and the equalizer. Generally, the DCCN performs consistently in simple flat fading channel and has advantages in low SNRs.

The BER of equalized DCCN receivers by SNR in frequency selective channel (3GPP EPA model [30]) is presented in Fig. 11(b). For BPSK and QPSK in middle to low SNR regimes ( $\leq 15\text{dB}$ ), equalized DCCN receivers still significantly outperform LS-Spline by mostly 1.8 to 2.3 dB w/o CP, and 2 to 3 dB w/ CP. However, when  $\text{SNR} \geq 18\text{dB}$ , the BER of equalized DCCN gradually reach a floor and underperforms the benchmark. For 8QAM and 16 QAM, however, the equalized DCCN only slightly outperforms the benchmark in low SNRs ( $\leq 9\text{dB}$ ), while significantly underperform the benchmark in middle to high SNRs ( $\geq 9\text{dB}$ ). Further examination shows there is systematic error in DCCN that causes the BER floor. It shows that in complex fading, the DCCN performs worse in high SNRs and higher modulation orders.



(a) Flat Fading



(b) Multipath Fading (3GPP-EPA [30])

Fig. 12. BER of Equalized DCCN Receiver in Rayleigh Channels, BPSK, benchmarked by expert OFDM receiver with Least Square channel equalizer.

In Figs. 12, the BER of equalized DCCN receivers with BPSK is further compared to equalizers with perfect channel state information, as well as LMMSE, LS-Linear, and LS-Spline estimators. In flat fading (Fig. 12(a)), for  $\text{SNR} \leq 13\text{dB}$ , equalized DCCN receivers w/o CP only slightly underperforms perfect equalizer by around 0.3 dB for DCCN (slightly outperform LMMSE based on perfect SNR by ignorable margin), while DCCN w/ CP slightly outperform perfect equalizer by about 0.5 dB. In EPA channel (Fig. 12(b)), for  $\text{SNR} \leq 13\text{dB}$ , the equalized DCCN receivers w/o CP underperforms the perfect equalizer (which is almost the same as LMMSE based on perfect SNR) by 0.5 to 1 dB, and DCCN w/ CP slightly outperforms perfect equalizer by up to 0.3 dB. It shows that DCCN is very close to perfect equalizer for BPSK without prior channel knowledge from middle to very low SNRs. On the other hand, both DCCN and LS-Linear equalizer exhibits BER floors, which implies that DCCN may belong to the family of linear but cubic interpolation.

Table V. Alternative Flow-Graphs of Basic DCCN Receiver without CP

| Original    | a  | b    | c    | d    | e      | f    | g    |
|-------------|----|------|------|------|--------|------|------|
| Batch Norm  | -  | -    | -    | -    | -      | -    | -    |
| Slice       | -  | -    | -    | -    | -      | -    | -    |
| 1D C-Conv   | FC | -    | -    | -    | -      | -    | FC   |
| Reshape     | -  | -    | -    | -    | -      | -    | -    |
| FC          | -  | -    | -    | -    | -      | -    | -    |
| IQ: Reshape | -  | -    | -    | -    | -      | -    | -    |
| R-Conv      | -  | none | none | none | -      | -    | none |
| R-Conv      | -  | none | none | none | -      | -    | none |
| Act0: LRelu | -  | -    | none | -    | -      | -    | -    |
| IQ, Act0    | -  | -    | IQ   | Act0 | -      | Act0 | -    |
| FC          | -  | -    | -    | -    | -      | -    | -    |
| LRelu       | -  | -    | -    | -    | linear | -    | -    |
| Reshape     | -  | -    | -    | -    | -      | -    | -    |
| Softmax     | -  | -    | -    | -    | -      | -    | -    |

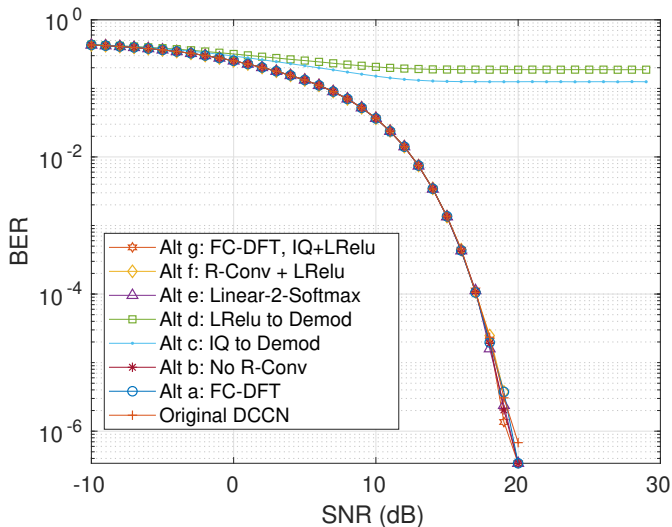


Fig. 13. Comparison of 7 Alternative Basic DCCN Receivers in AWGN Channel, 16QAM, benchmarked by expert OFDM receiver.

### C. Alternative Structures of Basic DCCN Receiver

To understand the contribution of layer(s) in the basic DCCN receiver, 7 alternative structures of the original model, (a–g), are explored by replacing and/or removing certain layer(s), as listed in Table V (– means the same as original).

The BER performance of the 7 alternative basic DCCN receivers for 16QAM are presented in Fig. 13. Similar results are found in 8QAM, while all alternatives perform identically well in BPSK and QPSK. Except *c* and *d*, rest of the alternatives performs almost identically to the original basic DCCN receiver. In alternatives *a* and *g*, the DFT-Like C-Conv layer in original model is replaced by a FC layer, the fact that *a* and *g* achieve the same performance of original DCCN implies that FC layer is able to perform DFT transformation as a C-Conv layer. In alternatives *b* and *g*, the R-Conv layers are removed, such that a combination of IQ data and LRelu-activated IQ data are fed into the last demodulation FC layer. They show that the R-Conv layers do not contribute to demodulation. However, R-Conv layers could accelerate the training. Alternative *e* shows that the last LRelu activation can be replaced by linear activation without harming performance. In alternatives *c* and

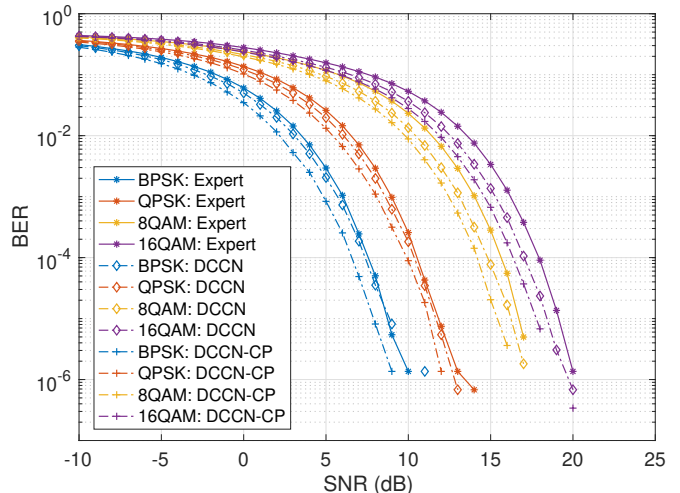


Fig. 14. Example of Inflated Performance: BER of basic DCCN Receiver in AWGN channel implemented by TensorFlow, where DCCN w/o CP consistently outperforms the benchmark. However, when cross-validated with noisy OFDM waveform generated in Matlab, its performance is similar to Fig. 10. Potential root causes could be the interferences between pseudo-random generator and training model due to the same platform and/or shared memory.

*d*, the R-Conv and the skip connection are removed so that either the IQ data (*c*) or LRelu-activated IQ data (*d*) are fed into the demodulation FC layer. The result shows that a FC layer could not perform demodulation based only on either IQ data or non-linear activated IQ data for higher modulation-order. Alternative *f* also removes the skip connection, but, R-Conv layers with  $2^m$  filters are in-place to pick out each constellation point. Alternative *f* shows that the R-Conv layers with non-linear activation could replace the skip connection.

### D. Cross Validation

In wireless communication, simulated channel model is often preferred over real channel in a limited environment since the former is considered more representative of environmental dynamics. Simulated channel model implemented by deep learning platforms, such as Tensorflow, brings training efficiency and convenience, especially with regards to back-propagation for autoencoders with both transmitter and receiver [6], [9]. However, in this paper, we found this practice may inflate the performance of trained model, which might be due to limited pseudo-random window of Tensorflow random generator, of which the random seeds could not be reset once flow graph is built. For example, in Fig. 14, our DCCN receivers without CP even outperform the Matlab benchmark, that tightly follows the theoretical limits. To avoid the risk of inflated performance, in [29], we provide a cross-validation platform, in which the received OFDM signal generated in Matlab is fed to the DCCN receiver implemented in Python, to get more trustable performance of our trained models.

## VI. CONCLUSION

In this paper, an OFDM receiver entirely based on Deep Complex Convolutional Networks (DCCN) is developed under

the guidance of signal processing structures of expert OFDM receiver. Compared to existing works, the Deep Neuron Networks developed in this paper contains not just dense layers followed by non-linear activations, but also several new components: complex convolutional layers, residual blocks, and skip connections. Moreover, the developed model is mostly linear and only contains a few non-linear activations necessary for demodulation, therefore, it does not contradict with well-established signal processing techniques. On the other hand, several sophisticated training techniques are employed to improve the training efficiency, including the logarithmic bit-error-rate in the loss function, exponential decay of learning rate, transfer learning for perpended module.

Without using explicit (Inverse) Discrete Fourier Transformations, the DCCN receiver achieves performance that is comparable to expert OFDM receiver in AWGN channel, and outperforms it in lower to middle SNR regimes of Rayleigh channels. Moreover, the DCCN learns to exploit the cyclic prefix in OFDM symbol to enhance its performance in AWGN, flat and multi-path fading channels. However, the developed DCCN model still under-performs the expert receivers in high SNR regime and higher modulation orders. Furthermore, the DCCN model is fairly general: its hyper-parameters especially with alternative structures  $b$  and  $g$ , are basically independent from the modulation order.

This work demonstrates that Deep Learning is able to learn complex transformations in base-band signal processing, and therefore could learn (and potentially create) advanced waveforms in wireless communications. It also shows that Deep Learning could potentially improve the performance of wireless system in low SNRs. However, more work is required to achieve better performance in high SNR regime, as well as for higher order modulations, such as structures for learning higher-order interpolations.

## REFERENCES

- [1] T. J. O'Shea, J. Corgan, and T. C. Clancy, "Convolutional radio modulation recognition networks," in *Engineering Applications of Neural Networks*, C. Jayne and L. Iliadis, Eds. Cham: Springer International Publishing, 2016, pp. 213–226.
- [2] T. J. O'Shea, L. Pemula, D. Batra, and T. C. Clancy, "Radio transformer networks: Attention models for learning to synchronize in wireless systems," in *2016 50th Asilomar Conference on Signals, Systems and Computers*, Nov 2016, pp. 662–666.
- [3] T. J. O'Shea, K. Karra, and T. C. Clancy, "Learning to communicate: Channel auto-encoders, domain specific regularizers, and attention," in *2016 IEEE International Symposium on Signal Processing and Information Technology (ISSPIT)*, Dec 2016, pp. 223–228.
- [4] T. O'Shea and J. Hoydis, "An introduction to deep learning for the physical layer," *IEEE Transactions on Cognitive Communications and Networking*, vol. 3, no. 4, pp. 563–575, Dec 2017.
- [5] T. J. O'Shea, T. Erpek, and T. C. Clancy, "Deep learning based MIMO communications," *CoRR*, vol. abs/1707.07980, 2017. [Online]. Available: <http://arxiv.org/abs/1707.07980>
- [6] S. Dorner, S. Cammerer, J. Hoydis, and S. ten Brink, "On deep learning-based communication over the air," in *2017 51st Asilomar Conference on Signals, Systems, and Computers*, Oct 2017, pp. 1791–1795.
- [7] T. Wang, C. Wen, H. Wang, F. Gao, T. Jiang, and S. Jin, "Deep learning for wireless physical layer: Opportunities and challenges," *China Communications*, vol. 14, no. 11, pp. 92–111, Nov 2017.
- [8] H. Ye, G. Y. Li, and B. Juang, "Power of deep learning for channel estimation and signal detection in ofdm systems," *IEEE Wireless Communications Letters*, vol. 7, no. 1, pp. 114–117, Feb 2018.
- [9] H. He, S. Jin, C.-K. Wen, F. Gao, G. Y. Li, and Z. Xu, "Model-driven deep learning for physical layer communications," 2018.
- [10] Q. Mao, F. Hu, and Q. Hao, "Deep learning for intelligent wireless networks: A comprehensive survey," *IEEE Communications Surveys Tutorials*, pp. 1–1, 2018.
- [11] C. Zhang, H. Zhang, D. Yuan, and M. Zhang, "Citywide cellular traffic prediction based on densely connected convolutional neural networks," *IEEE Communications Letters*, vol. 22, no. 8, pp. 1656–1659, Aug 2018.
- [12] Y. He, Z. Zhang, F. R. Yu, N. Zhao, H. Yin, V. C. M. Leung, and Y. Zhang, "Deep-reinforcement-learning-based optimization for cache-enabled opportunistic interference alignment wireless networks," *IEEE Transactions on Vehicular Technology*, vol. 66, no. 11, pp. 10433–10445, Nov 2017.
- [13] X. Li, J. Fang, W. Cheng, H. Duan, Z. Chen, and H. Li, "Intelligent power control for spectrum sharing in cognitive radios: A deep reinforcement learning approach," *IEEE Access*, vol. 6, pp. 25463–25473, 2018.
- [14] H. Huang, J. Yang, H. Huang, Y. Song, and G. Gui, "Deep learning for super-resolution channel estimation and doa estimation based massive mimo system," *IEEE Transactions on Vehicular Technology*, vol. 67, no. 9, pp. 8549–8560, Sept 2018.
- [15] K. Yang, M. C. Vuran, S. Scott, F. Guo, and C. R. Ahn, "Neural network-based channel estimation for 2x2 and 4x4 mimo communication in noisy channels," *International Balkan Conference on Communications and Networking*, May 2018. [Online]. Available: <http://par.nsf.gov/biblio/10075910>
- [16] M. Abadi et al., "TensorFlow: Large-scale machine learning on heterogeneous systems," 2015, software available from tensorflow.org. [Online]. Available: <https://www.tensorflow.org/>
- [17] F. Chollet et al., "Keras," <https://keras.io>, 2015.
- [18] A. Felix, S. Cammerer, S. Dörner, J. Hoydis, and S. ten Brink, "Ofdm-autoencoder for end-to-end learning of communications systems," *2018 IEEE 19th International Workshop on Signal Processing Advances in Wireless Communications (SPAWC)*, pp. 1–5, 2018.
- [19] J.-J. van de Beek, "Synchronization and channel estimation in ofdm systems," PhD dissertation, Lulea University of Technology, 1998.
- [20] Y. Shen and E. Martinez, "Channel estimation in ofdm systems," 2006.
- [21] Z. E. Ankaralı, B. Peköz, and H. Arslan, "Enhanced ofdm for 5g ran," *ZTE Communications*, vol. 15, no. S1, pp. 1–10, 2017.
- [22] W. Wang, M. Hu, J. Yi, H. Zhang, and Z. Li, "Improved cross-entropy-based tone injection scheme with structured constellation extension design for papr reduction of ofdm signals," *IEEE Transactions on Vehicular Technology*, vol. 67, no. 4, pp. 3284–3294, April 2018.
- [23] M. Kim, W. Lee, and D. Cho, "A novel papr reduction scheme for ofdm system based on deep learning," *IEEE Communications Letters*, vol. 22, no. 3, pp. 510–513, March 2018.
- [24] T. Y. Al-Naffouri and A. A. Quadeer, "Cyclic prefix based enhanced data recovery in ofdm," *IEEE Transactions on Signal Processing*, vol. 58, no. 6, pp. 3406–3410, June 2010.
- [25] J. Yang, Q. Guo, D. D. Huang, and S. Nordholm, "A factor graph approach to exploiting cyclic prefix for equalization in ofdm systems," *IEEE Transactions on Communications*, vol. 61, no. 12, pp. 4972–4983, December 2013.
- [26] S. Rathinakumar, B. Radunovic, and M. K. Marina, "Cpecycle: Recycling cyclic prefix for versatile interference mitigation in ofdm based wireless systems," in *Proceedings of the 12th International Conference on Emerging Networking EXperiments and Technologies*, ser. CoNEXT '16. New York, NY, USA: ACM, 2016, pp. 67–81.
- [27] L. Xu, J. Yang, D. Huang, and A. Cantoni, "Exploiting cyclic prefix for turbo-ofdm receiver design," *IEEE Access*, vol. 5, pp. 15762–15775, 2017.
- [28] C. Trabelsi, O. Bilaniuk, Y. Zhang, D. Serdyuk, S. Subramanian, J. F. Santos, S. Mehri, N. Rostamzadeh, Y. Bengio, and C. J. Pal, "Deep complex networks," in *International Conference on Learning Representations*, 2018. [Online]. Available: <https://openreview.net/forum?id=HIT2hmZab>
- [29] Z. Zhao, "Source code: An ofdm receiver based on complex deep neuron networks." [Online]. Available: [https://github.com/zhongyuanzhao/dl\\_ofdm](https://github.com/zhongyuanzhao/dl_ofdm)
- [30] "Evolved universal terrestrial radio access (e-utra): Base station (bs) radio transmission and reception (release 15)," 3rd Generation Partnership Project; Technical Specification Group Radio Access Network, 2018. [Online]. Available: <http://www.3gpp.org>